Soft Matter

PAPER

Cite this: *Soft Matter*, 2015, **11**, 3432

Transport of spherical colloids in layered phases of binary mixtures with rod-like particles

Mauricio Piedrahita, Alejandro Cuetos* and Bruno Martínez-Haya

Received 23rd December 2014
Accepted 6th March 2015

DOI: 10.1039/c4sm02865a

www.rsc.org/softmatter

The transport properties of colloids in anisotropic media constitute a general problem of fundamental interest in experimental sciences, with a broad range of technological applications. This work investigates the transport of soft spherical colloids in binary mixtures with rod-like particles by means of Monte Carlo and Brownian Dynamics simulations. Layered phases are considered, that range from smectic phases to lamellar phases, depending on the molar fraction of the spherical particles. The investigation serves to characterize the distinct features of transport within layers *versus* those of transport across neighboring layers, both of which are neatly differentiated. The insertion of particles into layers and the diffusion across them occur at a smaller rate than the intralayer diffusion modulated by the formation of transitory cages in its initial stages. Collective events, in which two or more colloids diffuse across layers in a concerted way, are described as a non-negligible process in these fluids.

I. Introduction

The thermodynamic and transport properties of multi-component systems constitute a key topic in Colloidal Science. The entropic contributions underlying the emergence of thermodynamically stable phases in mixtures of colloids of dissimilar shape (*e.g.* spherical, rod-like or disk-like particles) have been described in numerous computer simulations, and theoretical and experimental investigations.[1–13] Remarkably, phases arise that are inherent to the multicomponent nature of the systems and are therefore not present in the corresponding one-component fluids.

In this work, we present a simulation study of diffusion in layered liquid crystalline phases of binary mixtures of spherical and rod-like particles. Insights into diffusion processes in model systems of this kind are of fundamental interest for the general understanding of the behaviour of colloids and macromolecules in crowded environments. For instance, several studies have related the properties of sphere–rod colloidal systems to transport processes in cells, such as the self-diffusion of proteins in suspensions of F-actin,[14–17] the diffusion of globular macromolecules in lipid membranes,[18,19] or chromatin dynamics.[20]

The phase diagram of the sphere–rod binary system is relatively well known.[6–9] In contrast, the investigation of transport phenomena in these mixtures remains comparably scarce. Importantly, the transport properties of benchmark mono-component rod-like liquid crystals have been investigated previously. Löwen developed a general Brownian Dynamics (BD) algorithm that served to characterize the self-diffusion in liquid crystalline phases.[21] More recently, some theoretical[22] and computer simulation studies[23,24] unveiled specific aspects of the diffusion within layers and across layers in smectic phases of the pure fluid of rods. It seemed therefore timely to determine to which extent the diffusion behavior of pure systems can be extrapolated to binary mixtures.

The present investigation covers an ample range of molar fractions. On the one hand, at a low molar fraction of spheres ($x_s = 0.01$) the study basically explores the diffusion of isolated spheres in the smectic fluid of rods. Some fruitful incursions into the transport properties of this limiting case, in which the spheres can essentially be considered to be a tracer, have been performed in previous studies.[25–31] On the other hand, at the highest molar fraction of spheres included in our study ($x_s = 0.5$), a lamellar phase is formed that is characterized by alternate layers of rods and spheres, and the fluid presents novel features with respect to the pure rod fluid. Several rod elongations are as well explored in order to evaluate the influence of the layer thickness on the efficiency of the diffusion of the colloids across them.

Our study extends and revises qualitative aspects of the previous investigations of diffusion in sphere–rod mixtures away from the dilution limit,[32,33] and should therefore constitute an updated reference for the comprehension of transport in these systems. Specifically, a marked differentiation between the intralayer transport and the transport across layers is outlined. Furthermore, the importance of cooperative phenomena[24] in the diffusion of spheres through the layers of rods is investigated. This mechanism of transport is related to the enhanced local permeability of the layers that is induced once one sphere manages to penetrate into it, which triggers the concerted diffusion of neighbouring colloids.

Department of Physical, Chemical and Natural Systems, Universidad Pablo de Olavide, 41013 Seville, Spain. E-mail: acuemen@upo.es

The investigation has involved the extension of a Brownian Dynamics algorithm to the case of sphere–rod mixture, as well as the implementation of a dynamical criterium to probe collective transport events. The most relevant methodological aspects are described in Section 2, and the results are summarized and discussed in the subsequent sections of the paper.

II. Methodology

A. Interaction model

The spherical and the rod-like particles are represented as soft purely repulsive bodies, with the rods modelled as prolate spherocylinders. Within such framework, the interaction between any two particles is described *via* a shifted and truncated Kihara potential, according to the following expression:[34,35]

$$U_{ij} = \begin{cases} 4\varepsilon_{ij}\left[\left(1/d_{\mathrm{m}}^{*}\right)^{12} - \left(1/d_{\mathrm{m}}^{*}\right)^{6} + 1/4\right] & d_{\mathrm{m}}^{*} \le \sqrt[6]{2} \\ 0 & d_{\mathrm{m}}^{*} > \sqrt[6]{2} \end{cases} \quad (1)$$

here, U_{ij} is the interaction energy between two particles of species i and j (spheres or rods) and d_{m} denotes the minimum distance between the molecular cores of the pair of particles (the cylinder axis in the case of spherocylinders and the center of mass in the case of spheres). Obviously, d_{m} depends on the relative positions and orientations of the particles. The algorithm employed here to compute d_{m} for the only non-trivial case of a pair of spherocylinders is described in ref. 37. In eqn (1), $d_{\mathrm{m}}^{*} = d_{\mathrm{m}}/\sigma_{ij}$, where σ_{ij} represents the half-sum of the diameters of the two interacting particles. In this study, the same value for the diameter of spheres and rods is considered, *i.e.* $\sigma_{ij} = \sigma$. Hence, the rods are represented by a cylinder of length L capped by two hemispheres of diameter σ. This investigation considers such spherocylinders with elongations $L^{*} = L/\sigma = 4$, 5, and 7. The interaction is modulated by the energy parameter ε_{ij}. For the present work, we have assumed the same strength of the interaction for all pairs of particles (sphere–sphere, rod–rod and sphere–rod), hence $\varepsilon_{ij} = \varepsilon$.

B. Monte Carlo study of phase stability

The first stage of the study involved the construction of equilibrated configurations of the binary mixture in the layered state object of study. For this purpose, Monte Carlo simulations at constant number of particles, pressure and temperature (NPT-MC) were performed. The pressure and temperature are expressed in the reduced forms $P^{*} = P\sigma^{3}/k_{\mathrm{B}}T$ and $T^{*} = k_{\mathrm{B}}T/\varepsilon$ throughout the paper (k_{B} denoting the Boltzmann constant). Binary mixtures with molar fractions of spheres $x_{\mathrm{s}} = 0.01$, 0.1 and 0.5 were considered. The total number of particles employed in the simulations was at least $N \geq 2000$. The temperature of the system was fixed at the reduced value $T^{*} = 1.47$ in all simulations. At this temperature, the phase behaviour of the soft spherocylinder model resembles most closely the fluid of hard spherocylinders of the same length and diameter.[35,36]

The system was equilibrated with a long NPT simulation run (over 10^{6} MC cycles), and averages were subsequently computed over 2×10^{5} MC cycles, to characterize the thermodynamic and structural properties of the fluid. A MC cycle consists of N trials to move (rotation and/or translation) a randomly chosen particle, plus one attempt to change independently the three sides of the simulation box. The internal structure of the layered phase was monitored with the appropriate order parameters and distribution functions.[38]

Under the conditions of this study, the equilibration of the systems at high pressure resulted in layered arrangements, in which the spheres occupied the region in between the layers of rods. For each mixture, the pressure was adjusted to probe layered states with different packing fractions, $\eta = \rho(x_{\mathrm{s}}v_{\mathrm{s}} + x_{\mathrm{r}}v_{\mathrm{r}})$, where ρ is the number density, x_{s} and x_{r} are the molar fractions of spheres and rods, respectively, and $v_{\mathrm{s}}\sigma^{-3} = \pi/6$, $v_{\mathrm{r}}\sigma^{-3} = \pi/6 + \pi L^{*}/4$ their molecular volumes.

C. Brownian Dynamics

The second stage of the study was devoted to the computation of the dynamical properties of the mixtures. This was performed with Brownian Dynamics simulations at constant volume, started with the equilibrated configurations from the MC-NPT simulations described above. In BD simulations, the Langevin equation is integrated forward in time and trajectories of particles are created.[21,39]

For the spherical colloids, the position vector of particle j, $\mathbf{r}_j$, is updated in each BD step according to the expression:

$$\mathbf{r}_j(t + \Delta t) = \mathbf{r}_j(t) + \frac{D_0}{k_{\mathrm{B}}T}\mathbf{F}_j(t)\Delta t + (2D_0\Delta t)^{1/2}\mathbf{R}_0(t) \quad (2)$$

here, $D_0 = k_{\mathrm{B}}T/(\mu\sigma)$ is the self-diffusion coefficient of a single sphere, with μ being the viscosity of the solvent. $\mathbf{F}$ is the total force acting on sphere j due to other particles, and $\mathbf{R}_0$ is a random force with components sampled as to yield variance 1 and zero mean in the simulations. The time step was fixed at $\Delta t = 10^{-4}\tau$, with $\tau = \sigma^{2}/D_0$.

For the rod-like colloids, the position of the center of mass, $\mathbf{r}_j$, and the unitary vector defining the orientation of the particle, $\hat{\mathbf{u}}_j$, are updated in time by the following set of equations:

$$\mathbf{r}_j^{\parallel}(t + \Delta t) = \mathbf{r}_j^{\parallel}(t) + \frac{D_{\parallel}}{k_{\mathrm{B}}T}\mathbf{F}_j^{\parallel}(t)\Delta t + \left(2D_{\parallel}\Delta t\right)^{1/2}R^{\parallel}\hat{\mathrm{u}}_j(t) \quad (3)$$

$$\mathbf{r}_j^{\perp}(t + \Delta t) = \mathbf{r}_j^{\perp}(t) + \frac{D_{\perp}}{k_{\mathrm{B}}T}\mathbf{F}_j^{\perp}(t)\Delta t + (2D_{\perp}\Delta t)^{1/2}\left(R_1^{\perp}\hat{\mathbf{v}}_{j,1}(t) + R_2^{\perp}\hat{\mathbf{v}}_{j,2}(t)\right) \quad (4)$$

$$\hat{\mathrm{u}}_j(t + \Delta t) = \hat{\mathrm{u}}_j(t) + \frac{D_{\vartheta}}{k_{\mathrm{B}}T}\mathbf{T}_j(t) \times \hat{\mathrm{u}}_j(t)\Delta t + (2D_{\vartheta}\Delta t)^{1/2}\left(R_1^{\vartheta}\hat{\mathbf{w}}_{j,1}(t) + R_2^{\vartheta}\hat{\mathbf{w}}_{j,2}(t)\right) \quad (5)$$

where $\mathbf{r}_j^{\parallel}$ and $\mathbf{r}_j^{\perp}$ are the projections of $\mathbf{r}_j$ on the direction of $\hat{\mathbf{u}}_j$ and on the plane orthogonal to it, respectively. $\mathbf{F}_j^{\parallel}$ and $\mathbf{F}_j^{\perp}$ are the corresponding parallel and perpendicular components of the forces, and $\mathbf{T}_j$ is the total torque acting over particle j due

to the interactions with other particles of the fluid.[40] The Brownian motion of the particle is induced through the set of independent Gaussian random numbers (of variance 1 and zero mean), $R^{\parallel}$, $R_1^{\perp}$, $R_2^{\perp}$, R_1^{ϑ} and R_2^{ϑ}, and unitary random vectors perpendicular to $\hat{\mathbf{u}}_j$, denoted in the above equations as $\hat{\mathbf{v}}_{j,m}$ and $\hat{\mathbf{w}}_{j,m}$ ($m = 1, 2$).

The self-diffusion coefficients driving the Brownian Dynamics of the rods, $D_{\parallel}$, $D_{\perp}$ and D_{ϑ}, have been calculated with the analytical expressions proposed by Shimizu for prolate spheroids:[41]

$$\begin{aligned} D_{\perp} &= D_0 \frac{(2a^2 - 3b^2)S + 2a}{16\pi(a^2 - b^2)} b, \\ D_{\parallel} &= D_0 \frac{(2a^2 - b^2)S - 2a}{8\pi(a^2 - b^2)} b, \\ D_{\vartheta} &= 3D_0 \frac{(2a^2 - b^2)S - 2a}{16\pi(a^4 - b^4)} b, \end{aligned} \tag{6}$$

with

$$S = \frac{2}{(a^2 - b^2)^{1/2}} \log \frac{a + (a^2 - b^2)^{1/2}}{b}, \quad (a = (L + \sigma)/2, b = \sigma/2) \tag{7}$$

For the present study, several types of dynamical observables were computed for both spheres and rods, namely the mean square displacement (MSQD), and the self parts of the intermediate scattering function (SISF) and of the van Hove function (SVHF), as defined below.

Mean square displacements of the particles were computed along the three axes of the simulation box:

$$\delta_k = \left\langle (\Delta\mathbf{r})^2(t) \right\rangle_k = \left\langle \frac{1}{N_k} \sum_{j=1}^{N_k} \left(\mathbf{r}_j(t) - \mathbf{r}_j(0) \right)^2 \right\rangle, \tag{8}$$

where the delimiters $\langle \ldots \rangle$ denote the ensemble average and N_k is the number of particles of each species ($k \equiv r, s$). In addition, we computed the components of the mean square displacements of the particles in the directions parallel, $\delta_k^{\parallel} = \langle \Delta r_{\parallel}{}^2(t) \rangle_k$, and perpendicular, $\delta_k^{\perp} = \langle \Delta r_{\perp}{}^2(t) \rangle_k$, to the nematic director of the system of rods, which is coincident with the normal to the layers.

The self intermediate scattering function provides a measure of the structural relaxation of the density fluctuations and was evaluated for each component of the mixture, according to the expression:

$$F_k(\mathbf{q}, t) = \frac{1}{N_k} \left\langle \sum_{j=1}^{N_k} \exp\left[i\mathbf{q} \cdot \left(\mathbf{r}_j(t + t_0) - \mathbf{r}_j(t_0) \right) \right] \right\rangle, \tag{9}$$

where $\mathbf{q}$ is the wave vector calculated at the first peak of the rod static structure factor, which implies $|\mathbf{q}| = 2\pi/\sigma$, and $\mathbf{r}_j(t)$ are the particle positions at time t. Transverse and longitudinal relaxations may be defined as $F_k^{\perp}(t) = F_k(q_{\perp}, t)$ and $F_k^{\parallel}(t) = F_k(q_{\parallel}, t)$, respectively. These functions were calculated at the main peaks of the rod static structure factor, hence $q_{\perp} = 2\pi/\sigma$ and $q_{\parallel} = 2\pi/(L + \sigma)$.

An additional simple tool to study the non-continuous transport of particles through the layers of particles is the self-part of the van Hove function. To compare the inter-layer and intra-layer diffusion of the particles we have analyzed the components of this function, parallel and perpendicular to the nematic director defined as:

$$G_k^{\parallel}(r, t) = \frac{1}{N_k} \left\langle \sum_{i=1}^{N_k} \delta\left(r - \Delta r_{\parallel} \right) \right\rangle \tag{10}$$

$$G_k^{\perp}(r, t) = \frac{1}{N_k} \left\langle \sum_{i=1}^{N_k} \delta(r - \Delta r_{\perp}) \right\rangle \tag{11}$$

where, as mentioned above, the subscript k refers to the kind of particle, sphere or rod, and $\delta(-)$ denotes in this case the Dirac delta function. The SHVF can be understood as the probability density for a displacement r in a time interval t, along the directions parallel or perpendicular to the nematic director. Note that the SVHF is related to SISF by Fourier transform.

One specific aim of this work is to determine the importance of collective effects in the transport of spheres through the layers of rods.[23,24] For this purpose, we defined the following procedure to probe events of concerted diffusion of several particles across a layer. The jumps of spheres across layers are monitored on the $\hat{z}$ coordinate, which defines the displacements in the direction normal of the layers of rods. The initial time, t_i, and final time, t_f, of each jump for a given sphere j are defined as the closest instants where $|\hat{z}_j(t_f) - \hat{z}_j(t_i)| > L + \sigma$. For each jump, a particle n (sphere or spherocylinder) is defined as the *neighbour* of sphere j if, at t_i, the minimum distance between j and n is $d_m/\sigma < 6$. Being particle n a *neighbour* of j, it is also assigned as a *companion* of j in the diffusion process if $|\hat{z}_n(t_f) - \hat{z}_n(t_i)| > L/2$, which indicates that it has penetrated into the layer of rods within the (t_i, t_f) time interval. The frequency for events of concerted diffusion of a sphere with m companions through a layer is defined as $\omega_m = N_m/(tN_s)$, where N_s is the number of spheres and N_m is the number of jumps with m companions occurred during a simulation of time duration t. The total jump frequency for spheres is then given by $\omega = \sum_m \omega_m$.

Fig. 1 shows trajectories of two spheres and one rod involved in a typical event of collective diffusion. The concerted diffusion of the three particles through a layer of rods is visualized as a rapid change in their $\hat{z}$-coordinates (at $t/\tau \approx 750$ in this example). As a general behavior, it can be appreciated that the particles typically spend a long time within a layer and eventually undergo comparably a rapid diffusion once they manage to penetrate into a neighbouring layer. Nevertheless, penetration does not imply that the full crossing of the layer is necessarily accomplished, and 'frustrated' jumps are common. Several of such frustrated jumps are highlighted in Fig. 1.

III. Results and discussion

In order to describe the most salient features of the diffusion of spheres in the environment provided by the layered arrangement of the rods, we will consider in the first place the limiting case of high dilution. This situation is represented in this work by the mixture with the lowest molar fraction of spheres, namely

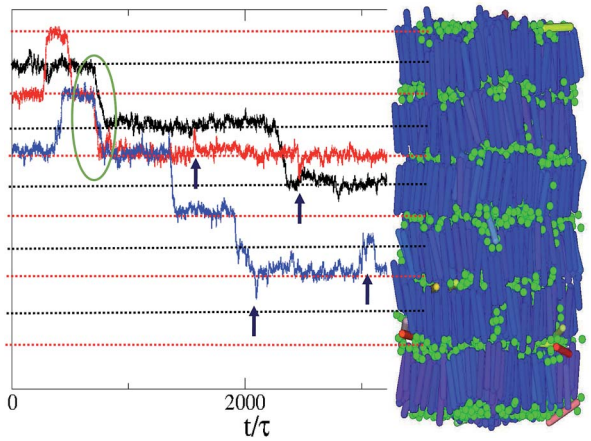

Fig. 1 Typical trajectories of two spheres (red and blue line) and one rod (black line) particles in a smectic phase. The $\hat{z}$-coordinate (vertical axis) describes the position of the particles along the normal of the layers. A snapshot of the smectic arrangement is provided next to the graph for clarity. Several rapid changes in $\hat{z}$, associated with jumps between layers can be appreciated in each trajectory. In addition, frustrated jumps in which a sphere or rod particle penetrates into the neighbouring layer of rods but eventually returns to its original layer are present. An event of collective motion of the two spheres and the rod takes place at $t/\tau \sim 750$, leading to a concerted change of layer of the three particles (see text for details).

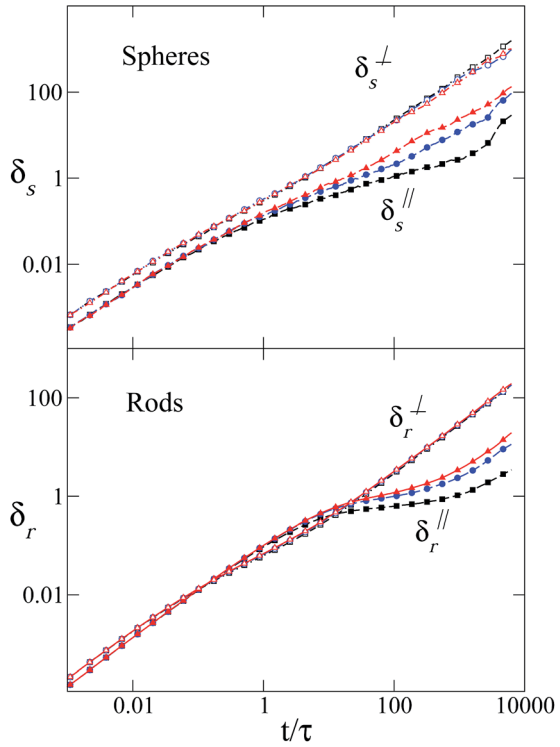

Fig. 2 Time evolution of the mean square displacements, $\delta^{\parallel}$ (solid symbols) and $\delta^{\perp}$ (open symbols), for spheres (top panel) and rods (bottom panel) in layered smectic states of binary mixtures with a low molar fraction of spheres ($x_s = 0.01$). In these fluids, the rods have $L^* = 7$ and smectic states with three different packing fractions are considered, namely $\eta = 0.564$ (black and squares), 0.537 (blue and circles) and 0.523 (red and triangles).

$x_s = 0.01$. Typical mean square displacements, self scattering functions and van Hove functions obtained within this regime are shown in Fig. 2–4. The directionality of the transport imposed by the layered arrangement is specifically exposed by representing the time evolution of the projections of those three magnitudes, parallel and perpendicular to the normal of the layers.

It can be appreciated that the MSQD functions of both rods and spheres evolve linearly at short times ($t/\tau < 1$, see Fig. 2). This is indicative of an initial regime of non-collisional diffusive dynamics, in which the absolute differences between $\delta^{\parallel}$ and $\delta^{\perp}$ are solely determined by geometrical constraints. At longer times, the MSQD deviates from linearity, giving rise to more or less pronounced plateaus due to the interaction of the particles with their nearest neighbors, and eventually enters a new regime of rapid growth as the particles diffuse past them.

Importantly, for the spheres, $\delta_s^{\perp}$ is greater than $\delta_s^{\parallel}$ throughout all temporal regimes, in some ranges by as much as one or several orders of magnitude, depending on the packing fraction of the system. The physical interpretation of this finding is that the spheres diffuse more efficiently within the region in between layers of rods with displacements parallel to the layer planes (intralayer transport), while their diffusion into the layers of rods (interlayer or across-layer transport) is comparably less favored. Moreover, while $\delta_s^{\perp}$ is weakly independent of the density of the smectic phase, at least within the time range represented in Fig. 2, $\delta_s^{\parallel}$ displays a clear dependence on density at sufficiently long times ($t/\tau > 1$).

In concordance with these features, $F_s^{\perp}$ decays rapidly to zero and remains roughly independent of the packing fraction of the system, while $F_s^{\parallel}$ follows a much slower decay and develops an extended plateau at times $t/\tau > 1$ with an appreciable dependence on the packing fraction. These observations indicate that the packing of the smectic layers determines to a large extent the penetrability of the spheres into the layers and their diffusion across them, but it does not affect so much the intralayer dynamics.

The marked anisotropy in the diffusion of spheres in the directions parallel and perpendicular to smectic layers is observed systematically for all the rod elongations and molar fractions of spheres studied in this work. While it seemed *a priori* plausible that differences between the diffusion in the two directions should exist, it must be mentioned that the present observations are in apparent contradiction with the only previous study that to our knowledge has considered transport in sphere–rod mixtures away from the dilution limit, carried out by Cinacchi and de Gaetani,[32,33] which concluded that spheres diffuse in a roughly isotropic way within a smectic phase of rods (that is, $\delta_s^{\perp} \approx \delta_s^{\parallel}$). The origin of this discrepancy remains unclear to us, as it seems unlikely that it is related to the different model that they employ to represent the rods, or to the fact that they use Molecular Dynamics instead of the Brownian Dynamics presently employed. To this respect, the present work should constitute a revised reliable reference for the rationalization of transport in rod–sphere colloidal mixtures.

The plateaus observed in the temporal evolution of $\delta^{\parallel}$ and $F^{\parallel}$ are indicative of a hindered relaxation in the direction along the

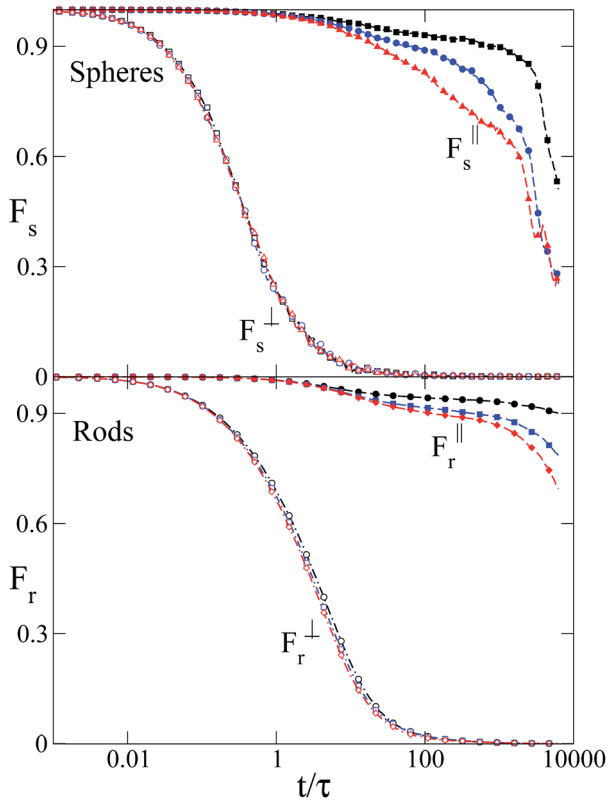

Fig. 3 Time evolution of the parallel and perpendicular projection of the self intermediate scattering function, $F_k^{\parallel}$ (solid symbols) and $F_k^{\perp}$ (open symbols), for spheres (top panel) and rods (bottom panel) for the same fluids and packing fractions shown in Fig. 2.

normal to the layers, in contrast to the smooth liquid-like behaviour found for the intralayer diffusion. Such behavior can be interpreted in terms of a glass-like behavior for the diffusion across layers, where the formation of transient cages preclude, or delay, the diffusion of the particles.[24]

The directionality in the diffusion is similarly followed by the rods that conform the smectic layers. Indeed, the long-time mobility of the rods within the layers is much more efficient than the diffusion out of the layer, as can be appreciated in the $\delta_r^{\perp}$ and $\delta_r^{\parallel}$ functions depicted in Fig. 2. In fact, the plateaus found for the $\delta_r^{\parallel}$ of the rods are much more pronounced than those displayed by $\delta_s^{\parallel}$ for the spheres in the binary mixture. This indicates that while both species are partially trapped in the interlayer space, the spheres escape from the cages easier than the rods.

Further noteworthy differences between the diffusion of rods and spheres arise at intermediate times. Whereas for spheres the parallel component of the MSQD remains smaller than the perpendicular one at all times, Fig. 2 shows that for rods there are two crossovers, leading to a broad time window in which $\delta_r^{\parallel} > \delta_r^{\perp}$. This transient behavior can be related to the slow down of the perpendicular diffusion due to the collision with other particles, while the free diffusive regime reaches longer times in the parallel direction. At longer times, the particles eventually feel the adjacent rod layer where $\delta_r^{\parallel}$ displays a pronounced plateau and hence becomes significantly smaller than $\delta_r^{\perp}$. The first of those crossovers is analogous to the one observed experimentally by Grelet *et al.*[42] for a monocomponent fluid of rod-like particles. The observation of the second of the crossovers found in our simulations would however involve significantly longer diffusion times than the ones spanned in those experiments.

Fig. 4 illustrates the diffusion behavior in terms of the self van Hove function. The SVHF of spheres and rods is represented for illustrative layered states of fluids with rods of $L^* = 5$ and molar fractions of spheres $x_s = 0.01$ and $x_s = 0.5$. The noisy aspect of the data for the spheres for $x_s = 0.01$ is a consequence of low concentration of these particles and the correspondingly poor statistics. The SVHF has a Gaussian shape if the diffusion can be explained according to Fick's law. This was found to be always the case for the transport of the particles within a given layer; $G_k^{\perp}$ (not shown) is systematically Gaussian-like in our simulations. In contrast, the projection of the SVHF in the direction parallel to the nematic director (*i.e.* along the normal to the layers), $G_k^{\parallel}$, shown in Fig. 4, evolves to an oscillatory shape that reflects the non-homogeneous nature of the diffusion across layers, where the particles stay long times within a layer, and eventually undergo comparably sudden jumps across neighbouring layers. $G_k^{\parallel}$ does maintain a Gaussian-like shape, both for rod and spheres, at short times. This is related to the rattling of the particles around the center of the layer that they occupy. At longer times, multiple peaks emerge that cover with time progressively longer distances and eventually conform a periodic pattern with maxima at $\pm(L^* + 1)$, $\pm 2(L^* + 1)$,… , reflecting the diffusion across layers. At long times, the intensities of all the peaks in $G_k^{\parallel}$ tend to even up to similar values, although this occurs more readily for the spheres than for the rods, consistently with their more efficient diffusion.

It is important to notice that the comparison of the fluids with $x_s = 0.01$ *vs.* $x_s = 0.5$ displayed in Fig. 4 indicates that the SHVF reaches longer distances more rapidly for the $x_s = 0.01$ case. Care must be taken when interpreting this result, since it does not reflect the effect of increasing the concentration of spheres, but it is rather related to the fact that the rod layers are more tightly packed and, hence, less permeable in the state of the $x_s = 0.5$ fluid. The reason for this is that the two states involved in the comparison have similar packing fractions (see figure caption). Consequently, the density of particles is actually significantly higher for the $x_s = 0.5$ case (the spheres having a significantly smaller molecular volume than the rods) and the packing of the rod layers is greater to compensate for the voids in the layers of spheres. It is shown below that the higher concentration of spheres in the binary mixture actually promotes transport by enhancing events of collective diffusion through the layers of rods.

We discuss now the effect of the elongation of the rod-like particles on the transport properties. Longer rods make thicker layers, which can be foreseen to affect diffusion across layers. A first insight into this expectation is provided in Fig. 5 which displays the frequency of jumps of spheres, across rod layers, ω, as a function of the packing fraction for mixtures with $x_s = 0.01$ and $L^* = 4$, 5 or 7 for the rods. For a given value of L^*, ω

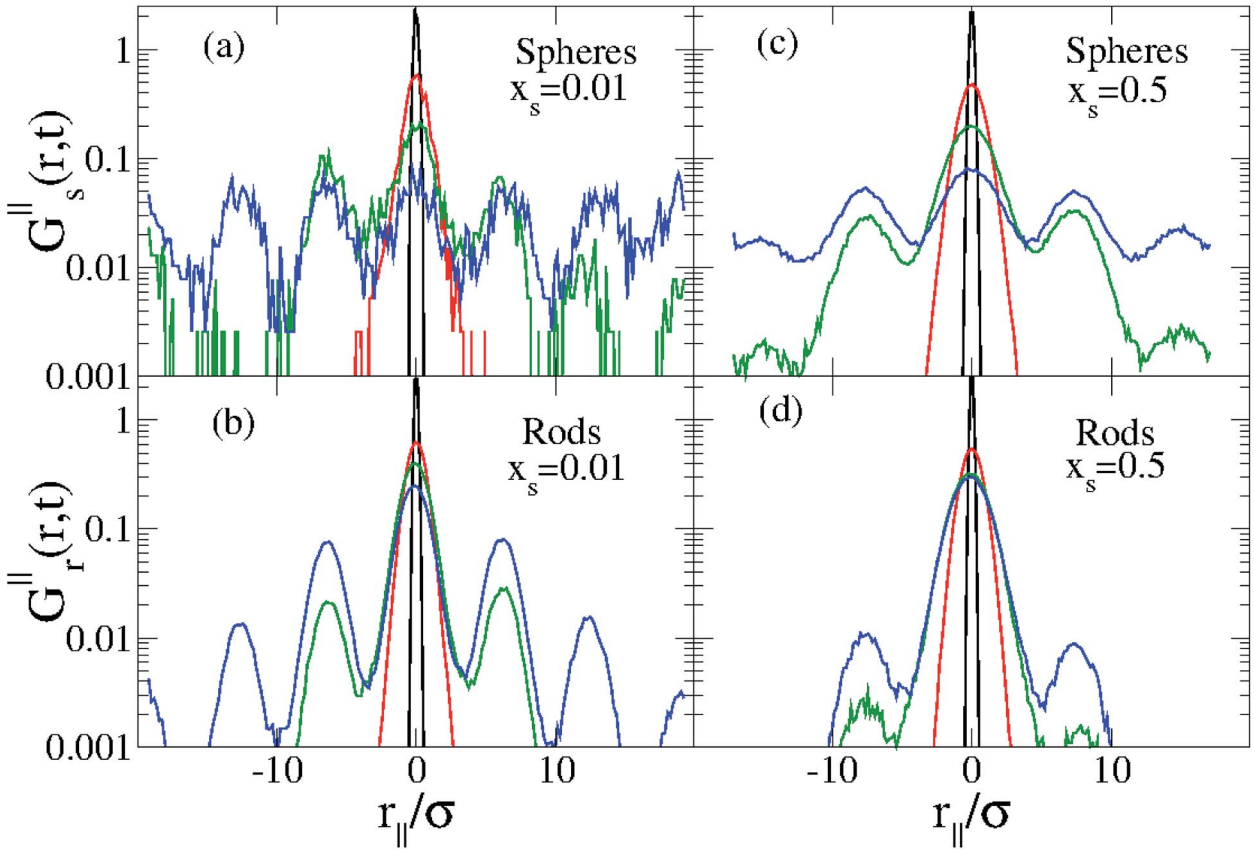

Fig. 4 Projection of the self van Hove function along the normal to the layers, $G_k^{\parallel}$, at different times for fluids of rods with $L^* = 5$. Panels (a) and (b) correspond to the limit of high dilution of spheres ($x_s = 0.01$, $\eta = 0.521$), while the panels (c) and (d) correspond to a lamellar arrangement ($x_s = 0.5$, $\eta = 0.536$). The curves plotted in each panel correspond to $t/\tau \approx 0.1$ (black), 10 (red) 1000 (green) and 5000 (blue). In each case, the top panel corresponds to spheres and the bottom one to rods. The diffusion across layers leads to a progressive reach of $G_k^{\parallel}$ to longer distances and the emergence of a periodic pattern of peaks reflecting the layer positions.

decreases steadily with increasing packing fraction, as a natural consequence of the reduced permeability of the denser rod layers. More importantly, for any given packing fraction, the frequency of jumps increases rapidly as the rod elongation is reduced. Indeed, it can be appreciated that ω for the fluid with $L^* = 4$ rods is about one order of magnitude larger than for the fluid with $L^* = 7$ rods.

Fig. 6 extends these insights with the mean square displacements for binary mixtures with rods of each of the three elongations. In this comparison, the overall packing fraction of the system is similar for the three systems, $\eta \approx 0.56$–0.57. The magnitude and the time evolution of $\delta_s^{\perp}$ for the spheres are weakly affected by the elongation of the rods, which seems to follow from the fact that the drift of the spheres within the interlayer environment can be considered to be sensitive to the tips of the rods and only indirectly to their length.[38] Opposite to this, the diffusion along the normal to the smectic layers changes substantially with rod elongation. The most relevant effect is related to a reduction in the plateau in $\delta_s^{\parallel}$ at long times as the rods become shorter, which is indicative of a sizeable enhancement of the crossing of spheres through the smectic layers. This observation can be attributed to two main aspects. First, the smectic layers of the shorter rods display a greater degree of defects and transient 'pores' which tend to facilitate the insertion of spheres. Second, for the thinner layers associated with the shorter rods, the probability of frustrated jumps is reduced. Indeed, once a sphere has penetrated into a smectic

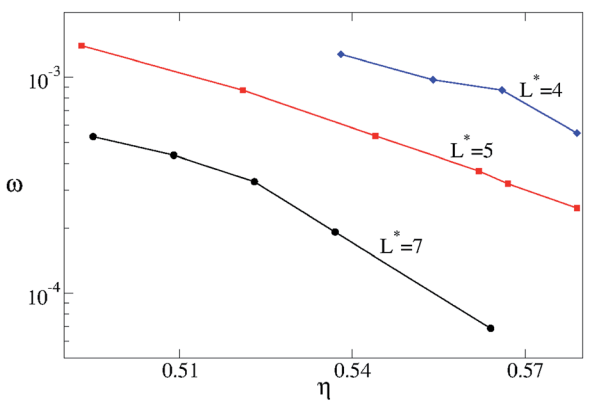

Fig. 5 Frequency of jumps of spheres across neighbouring layers of rods for fluids with rod elongations $L^* = 4$, 5 and 7. The molar fraction of spheres is $x_s = 0.01$ in all cases. The frequency of jumps decreases rapidly when either the packing fraction of the fluid or the elongation of the rods is increased.

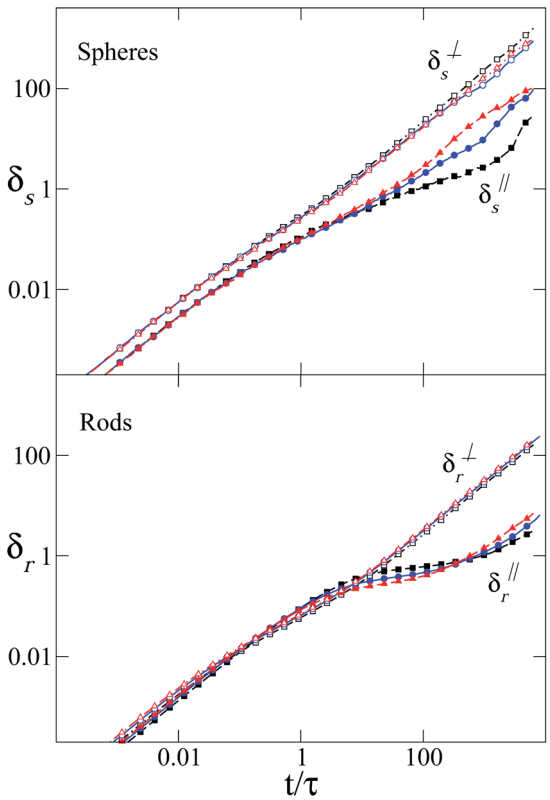

Fig. 6 Time evolution of the mean square displacements, $\delta^{\parallel}$ (open symbols) and $\delta^{\perp}$ (close symbols), for spheres (top panels) and rods (bottom panels) in layered phases of binary mixtures with rods of different elongations, $L^* = 4$ (red triangles), 5 (blue circles) and 7 (black squares), at a similar packing fraction (η = 0.566, 0.562 and 0.564, respectively).

layer, the probability and the readiness with which that sphere diffuses fully through it to the next inter-layer region are greater for the layers of shorter rods.

Interestingly, the evolution of $\delta_r^{\parallel}$ for the rods at the different values of L^* is qualitatively different than the one found for the spheres. For the rods, at intermediate times (within $t/\tau \approx 20$–200) the mean displacements are greater for the longer rods. In this regime, the MSQD is roughly equal to σ, meaning that the rods are in the process of attempting insertions into the neighbouring layers. This stage would be more efficient for the longer rods, presumably as a consequence of their greater degree of parallel orientation. At longer times, this trend reverses again to a situation similar to the one found for the spheres, due to the difficulty that encounter the rods to fully insert into the neighbouring layers as the layers become thicker.

We move on to discussing the relative importance of events of collective diffusion, which has been specifically investigated in this work as a transport mechanism intrinsic to layered liquid crystal phases. In a typical event of this type (see Fig. 1), the insertion of one sphere into the layer of rods opens a channel that triggers the diffusion of further neighboring particles (spheres or rods) that eventually move along through the layer in a concerted way. One particular question that our study aimed to answer was the influence that the molar fraction of spheres may have on this type of transport phenomena.

Fig. 7 depicts the relative frequencies of the jumps across layers in which the sphere that initiates the diffusion process crosses the layer of rods on its own, as well as those of the events in which it is accompanied by either just one particle (sphere or rod), or by two or more particles, in its drift through the rod layer. Results are shown for $x_s = 0.01$ mixtures with rods of each of the three elongation included in this study, $L^* = 4$, 5, 7, and for the mixture with $L^* = 5$ rods at the two additional molar fractions presently investigated, $x_s = 0.1$ and 0.5. For reach system, a range of packing fractions are included.

As a general trend, the importance of collective events decreases with increasing packing fraction, as a natural consequence of the reduced permeability of the layers of rods. Furthermore, the fraction of collective events also decreases appreciably (by up to one order of magnitude) as the rod elongation is increased from $L^* = 4$ to 7. This follows mainly from the enhanced probability of frustrated jumps as the layers of rods become thicker. Nevertheless, collective events can become dominant (meaning that more than half of the jumps involve at least one companion) in the smectic states of

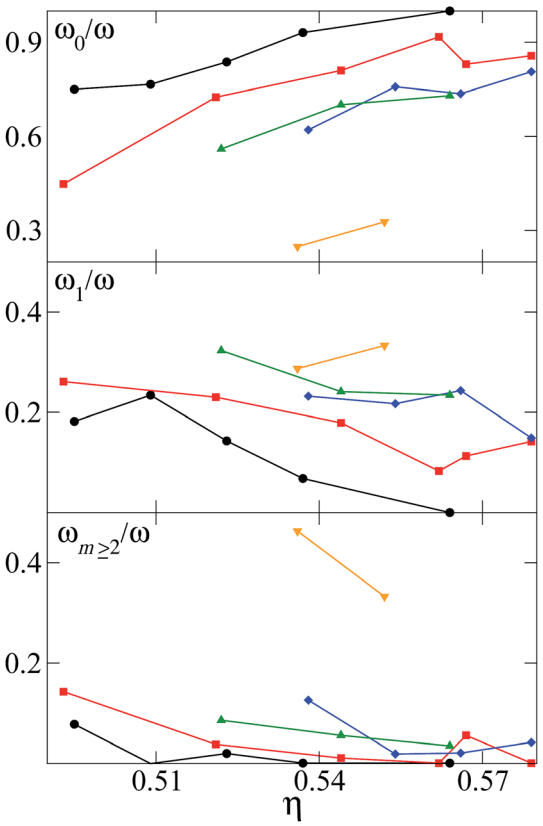

Fig. 7 Relative frequencies of jumps of spheres across neighbouring layers of rods for fluids with rod elongations and molar fraction of spheres (L^*,x_s): (7,0.01) black lines and circles, (5,0.01) red lines and squares, (4,0.01) blue lines and diamonds, (5,0.1) green line and up triangles, (5,0.5) orange lines and down triangles. The figure shows the fraction of jumps of single spheres without companions (ω_0/ω, top), spheres with one companion (ω_1/ω, middle), and spheres with two or more companions ($\omega_{m\geq 2}/\omega$, bottom).

lower density. Fig. 7 shows that, even in the dilution limit ($x_s = 0.01$), the relative frequency of jumps in which the sphere diffuses with no companions can be as low as ≈ 0.4 in the smectic states of lowest density investigated ($\eta < 0.5$), although it increases to higher values, even reaching 1.0 (no collective events detected), for the longest rods and highest densities investigated ($L^* = 7$, $\eta > 0.56$).

It seemed timely to introduce in this context the effect that increasing the molar fraction of spheres may have on collective diffusion. The enhanced presence of the spheres can be expected to disrupt the smectic structure, introducing defects due to steric effects induced, either by individual spheres or by the clustering of spheres in between the layers of rods. For this purpose, we have explored molar fractions up to values associated with the binary mixture equimolar in rods and spheres, $x_s = 0.5$, for which the smectic phase is replaced by a commensurable lamellar phase with a stable alternation of layers of rods and spheres. Specifically, three molar fractions, namely $x_s = 0.01$, 0.1 and 0.5, were investigated for the mixtures with rods of elongation $L^* = 5$.

Interestingly, the events of collective diffusion gain rapidly in importance as the molar fraction of spheres is increased and eventually become dominant at all packing fractions. For $x_s = 0.5$ (lamellar phase), the majority of jumps occur with at least one companion; in fact, the frequency for individual jumps of single spheres becomes smaller than 0.4, while the relative weight of the jumps with two or more companions reaches values close to 0.5 for the cases here investigated. A detailed inspection of the type of companions involved in the collective diffusion process revealed that in the limit of high dilution of spheres the companions are mostly rods; only less than 8% of the companions monitored in our simulations were spheres. The situation reverses dramatically as the molar fraction of spheres is increased: at $x_s = 0.1$ and 0.5, as many as *ca.* 45% and 75% of the companions, respectively, were spheres. Hence, it can be concluded that the microscopic mechanism driving collective transport, initiated by the insertion of spheres into the rod layers, changes qualitatively with the composition of the binary mixture: at low concentration of spheres, it promotes the exchange of rods between adjacent layers, while at high concentration of spheres, the process is dominated by the collective migration of the spheres themselves. The intermediate behaviour found at $x_s = 0.1$ suggests that a smooth switch between both regimes can be expected as the molar fraction of spheres is varied in the mixture.

IV. Conclusions

Diffusion in binary mixtures of spherical and rod-like particles shows a complex dynamic behavior, depending on factors such as the packing fraction, elongation of the rods or molar fraction of the mixture. In the layered phases investigated in this work, transport is clearly anisotropic. The faster contribution to the diffusion of spheres and rods arises from the direction perpendicular to the normal of the layers (intralayer diffusion), which is significantly more efficient than interlayer diffusion involving transport of particles across layers. The initial stages of interlayer diffusion of spheres display a glass-like behavior associated with the formation of transitory cages before potential penetration into the neighbouring layers occurs.[24]

Increasing the packing fraction of the fluid enhances the directionality of the transport, since it suppresses the diffusion across layers more efficiently than the inlayer component. Longer rods have a similar effect, as they give rise to thicker layers, for which frustrated attempts of particles to diffuse across them become more common.

Importantly, increasing the molar fraction of spheres promotes collective diffusion, involving the concerted transport of groups of particles through the layers of rods. Collective transport is typically seeded by the insertion of one sphere into a rod layer, thereby opening a channel that triggers the diffusion of further particles. This diffusion mechanism can be dominant under favorable conditions, namely a small packing of the system and/or a significant molar fraction of spheres.

Acknowledgements

The research activity of our group is currently supported by the Government of Spain, through projects CTQ2012-32345 and Consolider-Ingenio CSD2009-00038, and by Junta de Andalucía-FEDER through project P12-FQM-4938.

References

1 S. Asakura and F. Oosawa, *J. Polym. Sci.*, 1958, **32**, 183.
2 S. M. Oversteegen and H. N. W. Lekkerkerker, *J. Chem. Phys.*, 2004, **120**, 2470.
3 L. Harnau and S. Dietrich, *Phys. Rev. E: Stat., Nonlinear, Soft Matter Phys.*, 2004, **69**, 051501.
4 N. Doshi, G. Cinacchi, J. S. van Duijneveldt, T. Cosgrove, S. W. Prescott, I. Grillo, J. Phipps and D. I. Gittins, *J. Phys.: Condens. Matter*, 2011, **23**, 194109.
5 F. Gamez, R. D. Acemel and A. Cuetos, *Mol. Phys.*, 2013, **111**, 3136–3146.
6 Z. Dogic, K. R. Purdy, E. Grelet, M. Adams and S. Fraden, *Phys. Rev. E: Stat., Nonlinear, Soft Matter Phys.*, 2004, **69**, 051702.
7 A. Cuetos, B. Martínez-Haya, S. Lago and L. F. Rull, *Phys. Rev. E: Stat., Nonlinear, Soft Matter Phys.*, 2007, **75**, 061701.
8 M. Adams, Z. Dogic, S. L. Keller and S. Fraden, *Nature*, 1998, **393**, 349.
9 T. Koda, M. Numajiri and S. Ikeda, *J. Phys. Soc. Jpn.*, 1996, **65**, 3551.
10 A. Cuetos, A. Galindo and G. Jackson, *Phys. Rev. Lett.*, 2008, **101**, 237802.
11 A. Stroobants and H. N. W. Lekkerkerker, *J. Phys. Chem.*, 1984, **88**, 3669.
12 H. H. Wensink, G. J. Vroege and H. N. W. Lekkerkerker, *Phys. Rev. E: Stat., Nonlinear, Soft Matter Phys.*, 2002, **66**, 041704.
13 A. Galindo, A. J. Haslam, S. Varga, G. Jackson, A. G. Vanakaras, D. J. Photinos and D. A. Dunmur, *J. Chem. Phys.*, 2003, **119**, 5216.
14 S. Gorti and B. R. Ware, *J. Chem. Phys.*, 1985, **83**, 6449.

15 M. Arrio-Dupont, G. Foucault, M. Vacher, P. F. Deveaux and S. Cribier, *Biophys. J.*, 2000, **78**, 901.
16 A. S. Verkman, *Trends Biochem. Sci.*, 2002, **27**, 27.
17 I. Y. Wong, M. L. Gardel, D. R. Reichman, E. R. Weeks, M. T. Valentine, A. R. Bausch and D. A. Weitz, *Phys. Rev. Lett.*, 2004, **92**, 178101.
18 D. Chapman, *Ann. N. Y. Acad. Sci.*, 1966, **137**, 745.
19 A. Saric and A. Cacciuto, *Phys. Rev. Lett.*, 2012, **108**, 118101.
20 S. Mangenot, S. Keller and J. Radler, *Biophys. J.*, 2003, **85**, 1817.
21 H. Löwen, *Phys. Rev. E: Stat., Nonlinear, Soft Matter Phys.*, 1994, **50**, 1232.
22 M. Bier, R. van Roij, M. Dijkstra and P. van der Schoot, *Phys. Rev. Lett.*, 2008, **101**, 215901.
23 A. Patti, D. El Masri, R. van Roij and M. Dijkstra, *Phys. Rev. Lett.*, 2009, **103**, 248304.
24 A. Patti, D. El Masri, R. van Roij and M. Dijkstra, *J. Chem. Phys.*, 2010, **132**, 224907.
25 S. G. J. M. Kluijtmans, G. H. Koenderink and A. P. Philipse, *Phys. Rev. E: Stat., Nonlinear, Soft Matter Phys.*, 2000, **61**, 626.
26 G. H. Koenderink, S. Sacanna, D. G. A. Aarts and A. P. Philipse, *Phys.Rev. E: Stat., Nonlinear, Soft Matter Phys.*, 2004, **69**, 021804.
27 G. H. Koenderink, A. P. Philipse and S. G. J. M. Kluijtmans, *J. Phys.: Condens. Matter*, 2000, **12**, A339–A343.
28 B. Cichocki and M. L. Ekiel-Jezewska, *J. Chem. Phys.*, 2009, **130**, 214902.
29 K. Kang, J. Gapinski, M. P. Lettinga, J. Buitenhuis, G. Meier, M. Ratajczyk, J. K. G. Dhont and A. Patkowski, *J. Chem. Phys.*, 2005, **122**, 044905.
30 K. Kang, A. Wilk, J. Buitenhuis, A. Patkowski and J. K. G. Dhonta, *J. Chem. Phys.*, 2006, **124**, 044907.
31 B. Schulz, M. G. Mazza and C. Bahr, *Phys. Rev. E: Stat., Nonlinear, Soft Matter Phys.*, 2014, **90**, 040501.
32 G. Cinacchi and L. De Gaetani, *J. Chem. Phys.*, 2009, **131**, 104908.
33 G. Cinacchi and L. De Gaetani, *Phys. Rev. Lett.*, 2009, **103**, 257801.
34 A. Cuetos, B. Martínez-Haya, L. F. Rull and S. Lago, *J. Chem. Phys.*, 2002, **117**, 2934.
35 A. Cuetos, B. Martínez-Haya, S. Lago and L. F. Rull, *J. Phys. Chem. B*, 2005, **109**, 13729.
36 A. Cuetos and B. Martínez-Haya, *Mol. Phys.*, DOI: 10.1080/00268976.2014.996191
37 A. Cuetos and B. Martínez-Haya, *J. Chem. Phys.*, 2008, **129**, 214706.
38 S. Lago, A. Cuetos, B. Martínez-Haya and L. F. Rull, *J. Mol. Recognit.*, 2004, **17**, 417.
39 H. Pei, S. Allison, B. M. H. Haynes and D. Agustin, *J. Phys. Chem. B*, 2009, **113**, 2564–2571.
40 C. Vega and S. Lago, *J. Chem. Phys.*, 1990, **93**, 8171.
41 H. Shimizu, *J. Chem. Phys.*, 1962, **37**, 765.
42 E. Grelet, M. P. Lettinga, M. Bier, R. van Roij and P. van der Schoot, *J. Phys.: Condens. Matter*, 2008, **20**, 494213.

